

Economic and social consequences of human mobility restrictions under COVID-19

April 27, 2020

Giovanni Bonaccorsi¹, Francesco Pierri², Matteo Cinelli³, Francesco Porcelli⁴,
Alessandro Galeazzi⁵, Andrea Flori¹, Ana Lucia Schmidt⁶, Carlo Michele Valensise⁷,
Antonio Scala³, Walter Quattrociocchi⁶, Fabio Pammolli^{1,8}

¹ Impact, Department of Management, Economics and Industrial Engineering, Politecnico di Milano

² Department of Electronics, Information and Bioengineering, Politecnico di Milano

³ CNR-ISC

⁴ Department of Law, Università di Bari

⁵ Department of Information Engineering, Università di Brescia,

⁶ Department of Environmental Sciences, Informatics and Statistics, Università Ca'Foscari di Venezia

⁷ Department of Physics, Politecnico di Milano

⁸ CADS, Joint Center for Analysis, Decisions and Society, Human Technopole,

* To whom correspondence should be addressed; E-mail: giovanni.bonaccorsi@polimi.it

In response to the COVID-19 pandemic, several national governments have applied lockdown restrictions to reduce the infection rate. We perform a massive analysis on near real-time Italian mobility data provided by Facebook to

investigate how lockdown strategies affect economic conditions of individuals and local governments. We model the change in mobility as an exogenous shock similar to a natural disaster. We identify two ways through which mobility restrictions affect Italian citizens. First, we find that the impact of lockdown is stronger in municipalities with higher fiscal capacity. Second, we find a segregation effect, since mobility restrictions are stronger in municipalities for which inequality is higher and where individuals have lower income per capita. Our results highlight the necessity of asymmetric fiscal measures to avoid a further increase in poverty and inequality induced by the lockdown.

Introduction

On March 9th 2020, Italy was the first European country to apply a national lockdown (1) in response to the spread of novel coronavirus (COVID-19) outside China borders. Following Italy and China, national lockdowns have been adopted by other governments, and mobility flows have been drastically reduced to lessen the reproduction rate of COVID-19 (2).

Increasing concerns are arising on the economic consequences of lockdown and how it can disproportionately affect the weaker and the poorer (3). Policy restrictions imposed by lockdown measures have determined a detrimental effect on several production sectors, heavily deteriorating global value chains and trade exchanges, motivating governments to announce fiscal interventions of about \$8 trillion and massive monetary measures from the G20 and others (4). Supply shocks can, in fact, trigger variations in aggregate demand that ultimately can be even larger than the COVID-related shocks themselves, hence imposing to immediately incorporating principles of system resilience to systemic disruption in order not to condition the future socio-economic recovery for the next decade (5–8).

The intensity of the sudden stop induced by the Covid-19 outbreak produces effects which are similar to those produced by a large scale natural disaster (9–13). Here, analogously to the literature on the economic damages of natural disasters (9, 14, 15), we model the change in mobility affecting Italian municipalities as an exogenous shock. We leverage a de-identified

large-scale collection of near real-time data provided by Facebook platform to characterize the effect of population mobility restrictions (16). On economic data, we rely on official statistics at highest available level of resolution, i.e. municipalities, to investigate the features of those who are mostly affected.

To understand how the lockdown measures impact on the economy, we rely as a proxy for economic downturn on mobility variations between and within italian municipalities across the deployment of the lockdown announcement. As shown in (2), mobility trends have reduced in fact by more than 90% in Italy after the lockdown, both in the retail and tourism sectors and in the service one, and this disruption of the mobility toward the workplace supports the use of mobility flows as a proxy of economic damages. Furthermore, we want to investigate the geographic distribution of the shocks in order to identify the economic conditions of the most and least affected zones. Rather than a homogeneous distribution we find, on the one side, that mobility reduction induced by lockdown is stronger for municipalities with higher fiscal capacity. On another side, we find that the contraction in mobility is higher for municipalities with lower per capita income and for those with higher inequality. In the aftermath of the crisis, central governments need not only to sustain economic recovery, but also to compensate the loss of local fiscal capacity, while channeling resources to mitigate the impact of lockdown on poverty and inequality.

Results and Discussion

Mobility restrictions

In Figs. 1A-B we compare two daily snapshots of the mobility network of municipalities aggregated at province level. After 21 days of national lockdown, we notice a striking fragmentation of the usual national mobility pattern from North to South. We characterize daily connectivity patterns (17) through network measures (18, 19).

In Fig. 1C, we analyze the temporal evolution of the number of the weakly connected components and the size of the largest connected component in the overall mobility network. We identify two opposite and significant trends, respectively increasing (Mann-Kendall (M-K): $P \sim 0$; Kendall's Tau (K-T): $P \sim 0$ $R = 0.64$; Theil-Sen (T-S): $R = 30.52$) and decreasing (M-K: $P \sim 0$; K-T: $P \sim 0$, $R = -0.67$; T-S: $R = -58.58$), that confirm the breakdown of hubs and long-range connections. We further assess the impact of mobility restrictions leveraging a network-based representation of mobility data and computing the network efficiency (Materials and Methods). Efficiency (20) is a good proxy of the system dynamics at play. Indeed, it is a global network measure that combines the information deriving from the network cohesiveness and the distance among the nodes and it measures how efficiently information/individuals may travel over the network (21). Additionally, it is particularly suitable for treating graphs with multiple components that evolve over time (22). As shown in Fig. 2, we observe a drastically decreasing trend of the efficiency (M-K: $P \sim 0$; K-T: $P \sim 0$, $R = -0.75$; T-S: $R = -0.00003$) that confirms a pronounced drop in the mobility potential of the network. Finally, we observe significant changes in the distribution of several node centrality measures over time (Materials and Methods, Figs.S1 to S9), with the most peripheral municipalities being those most affected by the lockdown.

In the following, we use the variation in Nodal Efficiency (Material and Methods), that is the contribution of each node to the global network efficiency, as a proxy for the effects of mobility restrictions. We compute the percentage relative change induced by the lockdown, by constructing mobility networks in two windows, 15 days before and after the day of intervention.

Mobility lockdown and economic segregation

Economic indicators

First, we focus on average individual Income, which constitute the base for the Italian Personal Income Tax declared annually by taxpayers, as a measure of private resources available to individuals.

Second, we use a municipal composite index of material and social well-being (Index of Socio-economic Deprivation) produced by the Italian Ministry of Economy and Finance, which aggregates several dimensions of lack of material and social well-being at municipal level (23, 24) (see Materials and Methods), representing one of the determinants of municipal standard expenditure needs.

In Fig. 3 we show the relationships between the two indexes with respect to the relative change in Nodal Efficiency. We observe a significant correlation, negative with the Deprivation Index (Pearson: $R = -0.153$, $P \sim 0$; S-R: $R = -0.235$, $P \sim 0$; T-S: $R = -0.064$; K-T: $R = -0.162$, $P \sim 0$) and positive with Income per Capita (Pearson: $R = 0.263$, $P \sim 0$; S-R: $R = 0.404$, $P \sim 0$; T-S: $R = 0.001$; K-T: $R = 0.273$, $P \sim 0$). We also notice similar and significant relationships using other network centrality measures (Table S3).

As a third main variable, we consider the level of municipal Fiscal Capacity, measured each year by the Italian Ministry of Economy and Finance and employed in the fiscal equalization process. Municipalities with high Fiscal Capacity tend to be financially independent from central government to fund local expenditures.

Finally, as additional regressors, we use a measure of municipal Inequality, i.e. the ratio between mean and median individual income, and an inverse measure of Urban Density in terms of the number of Real Estates per Capita.

Economic segregation from mobility disruption

In Fig. 4 we show the geographic distributions of the median Income per Capita of Italian provinces, separating the most affected (4a) from the least affected (4b). Additionally we report their distribution of Inequality with respect to the mean Inequality among all provinces. It is immediate to see that the most affected provinces have on average a lower Income per Capita. However the geographic distribution does not reflect a North-South divide but rather a separate dynamic of mobility for the North-East of Italy with respect to the rest of the country. Following this, among the most affected provinces there are also some of the richer provinces in the North-West, such as Turin and Genoa. Finally Income Inequality is greater than average in almost all the least affected provinces while in the most affected ones we have a more sparse distribution, which may be correlated with higher mobility disruptions. This suggests the necessity of a more detailed analysis at municipal level to qualify these aggregated results.

A second preliminary evidence is that the joint distribution by percentiles of the variation of mobility and economic indicators is concentrated on the top and bottom percentiles (SI Appendix, Figs. S12-S13). This result is important, since it shows a different relation between the extremes of the distribution of economic indicators and mobility with respect to the one observed around the mean (Fig. 3).

Against that background, in Table I we show the results of a quantile regression, where the relative variation in Nodal Efficiency over time is regressed against a set of economic regressors with regional controls. The quantile regression approach relaxes the assumptions of linear regressions and estimates the conditional quantile of a dependent variable over its predictors instead of conditioning on the mean (25). This allows us to concentrate on the dynamic at the tails of the distribution and to capture effects that with linear methods would otherwise seem insignificant (9). Indeed our estimates at the top and bottom quantile of the distribution of the variation in Nodal Efficiency show a better fitting with respect to the OLS ones reported as

reference in Table I

We observe a significant and positive relation between change in mobility during the lockdown and average individual Income for the bottom quantiles of the distribution. We study how municipalities at the lower end of the distribution of changes in mobility (10th-20th percentiles) are distributed according to their Income per Capita, and we find that the reduction in connectivity and mobility is higher for municipalities with a low average individual Income, while municipalities with high Income per Capita experience less intense changes. Moreover, at the upper end of the distribution, the relation is reversed. This asymmetry of the joint distribution of mobility contraction and Income per Capita unravels the existence of a possible segregation effect: even though some of the richer urban centers have experienced greater casualty rates, low income individuals are more affected by the economic consequences of the lockdown.

When we move to the analysis of municipal characteristics, measured through Deprivation and Fiscal Capacity, we find a different result: municipalities relatively richer in terms of social indicators and availability of own financial resources are those more hit by the loss in mobility efficiency in the aftermath of the lockdown. In other words, municipalities which experience the strongest effect of the lockdown are those with higher Fiscal Capacity and lower aggregate Deprivation.

Two seemingly opposite patterns emerge: individual indicators (average Income) show that the poorest are those more exposed to the economic consequences of the lockdown; on the contrary, aggregate indicators at the level of municipalities, i.e. Deprivation and Fiscal Capacity, reveal that richer municipality are those more hit by mobility contraction induced by the lockdown.

In order to shed light on these apparently contrasting results we look at the relationship between Inequality and the mobility contraction: we find a significant and negative relationship between the two variables at the lower end of the distribution of mobility reduction (10th-20th

percentiles).

This result further characterizes our findings: not only stronger negative changes in mobility are associated with low income municipalities but they are also linked to high level of inequality. This happens together with a lower level of the Deprivation Index and the high level of Fiscal Capacity and introduce an important additional detail: the distribution of income. By controlling for all these factors, we finally see that municipalities most severely affected are those where economic distances among individuals are still significant and hence where an erosion of the supply of public services will have a greater impact.

Our results are not affected by the inclusion of real estate and regional controls. We find a negative relation between the number of building per capita and changes in mobility: municipalities affected more by the contraction in mobility have more buildings per capita, hence less Urban Density. Moreover by including controls for all regions our results are not altered, which confirms that our findings are not driven by the regional distribution of municipalities.

All in all, our evidence shows that the lockdown seems to produce an asymmetric impact, hitting poor individuals within municipalities with strong fiscal capacity in all the country, with weaker effects in the rich provinces of the north-eastern Italy.

Conclusions

We analyze a massive mobility dataset before and after the Italian lockdown introduced to face the COVID-19 pandemic. We explore how variations in mobility relate to some fundamental economic variables, and we accordingly show that reduction in connectivity tends to be stronger for municipalities with low average individual Income and high income Inequality. At the same time, we notice that mobility restrictions have a higher impact on municipalities with higher Fiscal Capacity.

Our findings shed light on some social and economic consequences of policy measures

adopted to contain the diffusion of COVID-19. First, the lockdown seems to unevenly affect the poorer fraction of the population. On another side, we find that the reduction in mobility and connectivity induced by the lockdown is more pronounced for municipalities with stronger Fiscal Capacity. Finally, the distribution of income plays a role: municipalities where inequality is greater have experienced more pronounced mobility reductions.

Our results suggest the necessity of asymmetric fiscal measures. Emergency grants should be channeled soon to support consumption of the poor. In the absence of targeted lines of intervention, the lockdown would most probably induce a further increase in poverty and inequality.

References and Notes

1. Decreto del Presidente del Consiglio dei Ministri, *Gazzetta Ufficiale* **62** (2020).
2. Google, Covid-19 community mobility report (2020).
3. D. L. Jennifer Valentino-DeVries, G. J. Dance, Location data says it all: Staying at home during coronavirus is a luxury, <https://www.nytimes.com/interactive/2020/04/03/us/coronavirus-stay-home-rich-poor.html> (2020).
4. K. Georgieva, *International Monetary Fund, Speech April 9th* (2020).
5. R. M. Anderson, H. Heesterbeek, D. Klinkenberg, T. D. Hollingsworth, *The Lancet* **395**, 931 (2020).
6. A. Atkeson, What will be the economic impact of covid-19 in the us? rough estimates of disease scenarios, *Tech. rep.*, National Bureau of Economic Research (2020).
7. V. Guerrieri, G. Lorenzoni, L. Straub, I. Werning, Macroeconomic implications of covid-19: Can negative supply shocks cause demand shortages?, *Tech. rep.*, National Bureau of Economic Research (2020).

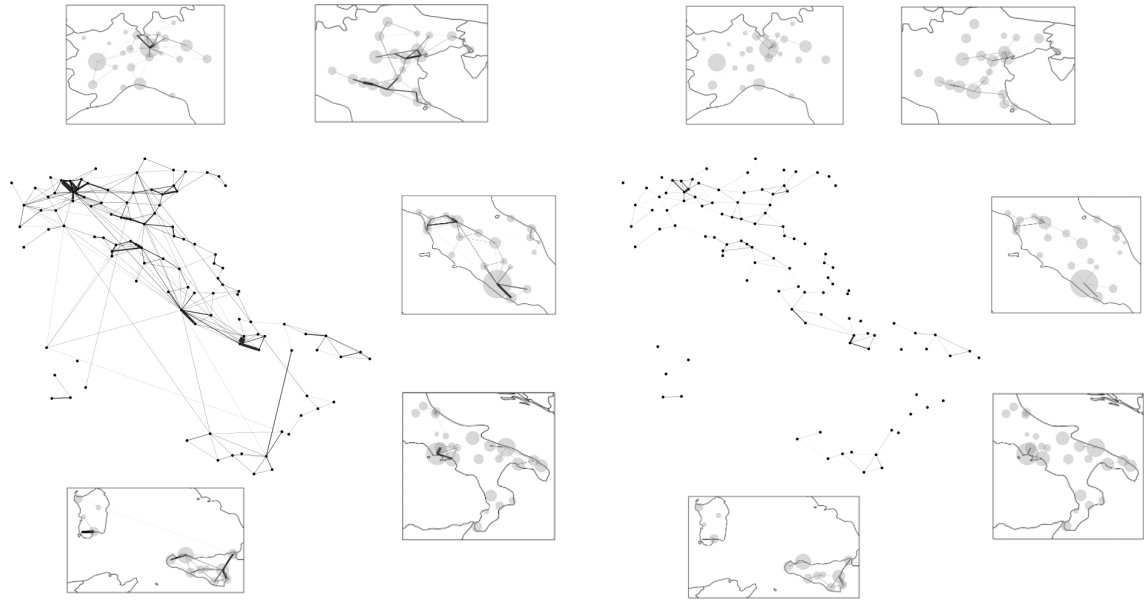
8. OECD, *New Approaches to Economic Challenges (NAEC)* (2020).
9. M. Coronese, F. Lamperti, K. Keller, F. Chiaromonte, A. Roventini, *Proceedings of the National Academy of Sciences* **116**, 21450 (2019).
10. V. M. Carvalho, M. Nirei, Y. U. Saito, A. Tahbaz-Salehi, *Supply Chain Disruptions: Evidence from the Great East Japan Earthquake*, no. ron287 in Discussion papers (2016).
11. A. Bunde, J. Kropp, H.-J. Schellnhuber, *The Science of Disasters: Climate Disruptions, Heart Attacks, and Market Crashes* (Springer Science and Business Media, 2012). Google-Books-ID: 7QH9CAAAQBAJ.
12. C. E. Boehm, A. Flaaen, N. Pandalai-Nayar, *The Review of Economics and Statistics* **101**, 60–75 (2018).
13. H. Inoue, Y. Todo, *Nature Sustainability* **2**, 841–847 (2019).
14. I. Noy, *Journal of Development economics* **88**, 221 (2009).
15. D. K. Kellenberg, A. M. Mobarak, *Journal of urban economics* **63**, 788 (2008).
16. P. Maas, *et al.*, *Proceedings of the 16th International Conference on Information Systems for Crisis Response and Management (ISCRAM), Valencia, Spain. 2019* (2019).
17. C. O. Buckee, *et al.*, *Science* (2020).
18. A.-L. Barabási, *et al.*, *Network science* (Cambridge university press, 2016).
19. M. Newman, *Networks* (Oxford university press, 2018).
20. V. Latora, M. Marchiori, *Physical review letters* **87**, 198701 (2001).
21. P. Crucitti, V. Latora, S. Porta, *Physical Review E* **73**, 036125 (2006).

22. E. Bullmore, O. Sporns, *Nature reviews neuroscience* **10**, 186 (2009).
23. Soluzioni per il Sistema Economico S.p.a (SOSE), Revisione della metodologia dei fabbisogni standard dei comuni, http://www.mef.gov.it/ministero/commissioni/ctfs/documenti/Nota_revisione_metodologia_FS2017_SOSE_13_settembre_2016.pdf (2016).
24. N. Caranci, *et al.*, *Epidemiologia E Prevenzione* **34**, 167 (2010).
25. R. Koenker, K. F. Hallock, *Journal of Economic Perspectives* **15**, 143–156 (2001).

Acknowledgements

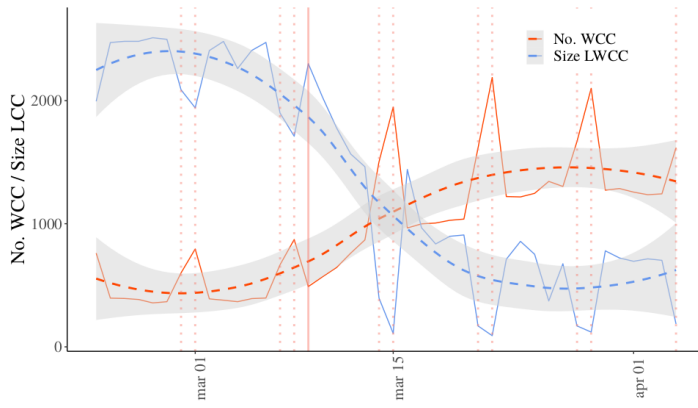
Funding: A.S., A.F, G.B, F.PI, M.C. and W.Q. acknowledge the support from CNR P0000326 project AMOFI (Analysis and Models OF social media) and CNR-PNR National Project DFM.AD004.027 "Crisis-Lab". **Authors contributions:** F.PI, AL.S, A.G, CM.V collected data; G.B, F.PI, M.C, A.G, A.S, CM.V, F.PO analyzed data; G.B, F.PI, M.C, A.F, W.Q, F.PA wrote the paper; W.Q, A.S, F.PA supervised the work. **Competing interests:** authors have no competing interests, this should also be declared. **Data and materials availability:** All data are made available for researcher to reproduce the result. Except for Facebook mobility data. This data was given in a previous agreement with Facebook.

Figures



(A) February 24th

(B) March 30th



(C) Temporal evolution of network connectivity

Figure 1: Connectivity of the Italian mobility network during COVID-19 epidemic.

We provide a snapshot of the mobility network on two Mondays before and after national lockdown (9th March), respectively on February 24th (A) and March 30th (B). Nodes represent municipalities aggregated at province level, and they all have equal size, whereas thickness of edges is proportional to the weight. Inserts provide an outlook on different regions, where node size is instead proportional to the population of the province. Figure (C) represents the temporal evolution of the network connectivity in terms of number of weakly connected components (No. WCC, red) and size of the giant connected component (Size LWCC, blue), measured on daily snapshots of the mobility network since 23th February. To visualize trends, we show a LOESS regression (dotted line) with 95% CI (shaded area), and highlight lockdown and week-days respectively with a solid and dotted vertical red lines. Trends are respectively significant increasing (M-K: $P \sim 0$; K-T: $P \sim 0$, $R = 0.64$; T-S: $R = 30.52$) and decreasing (M-K: $P \sim 0$; K-T: $P \sim 0$, $R = -0.67$; T-S: $R = -58.58$).

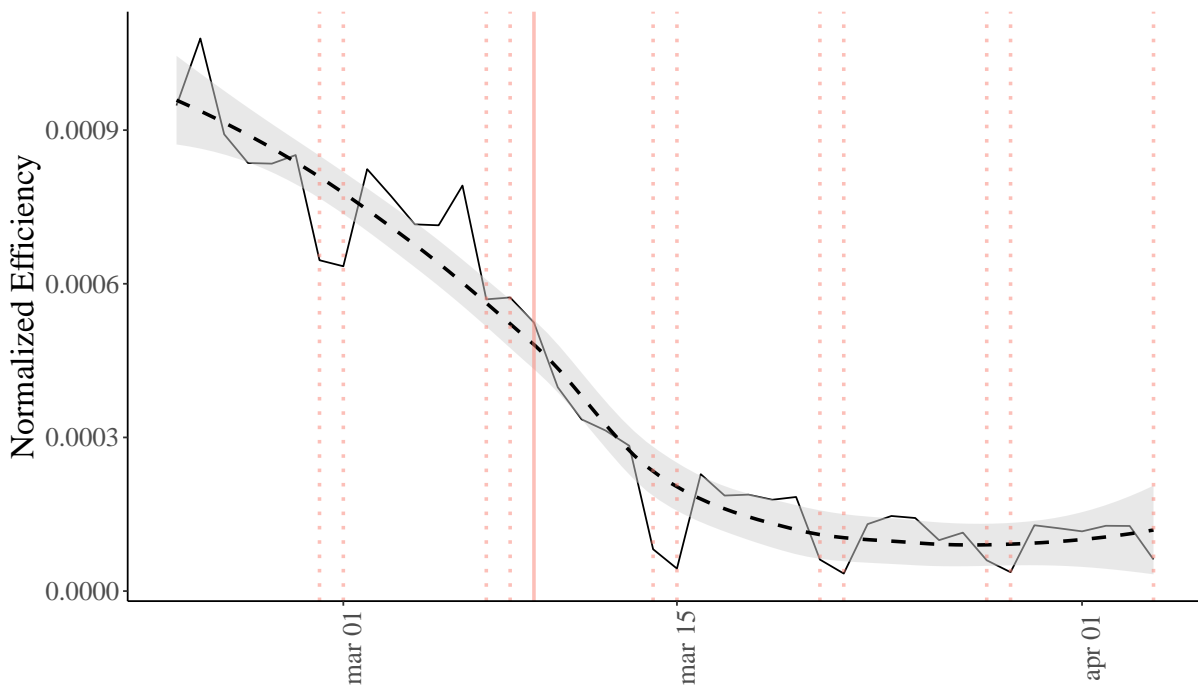


Figure 2: Efficiency of the Italian mobility network during COVID-19 epidemic.

Temporal evolution of the global efficiency for the Italian mobility network from February 23rd to April 4th. Efficiency is computed according to (20). We use the reciprocal of weights to model distances between nodes. To visualize the trend, we show a LOESS regression (dotted line) with 95% CI (shaded area), and highlight lockdown and week-days respectively with a solid and dotted vertical red lines. The trend is significantly decreasing (M-K: $P \sim 0$; K-T: $P \sim 0$, $R = -0.75$; T-S: $R = -0.00003$).

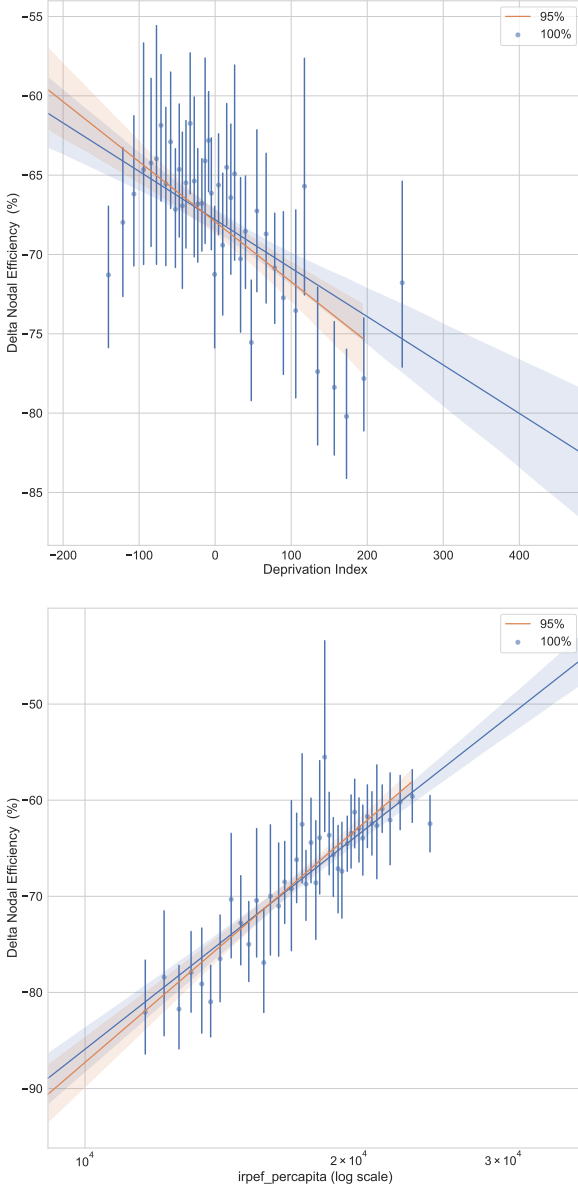
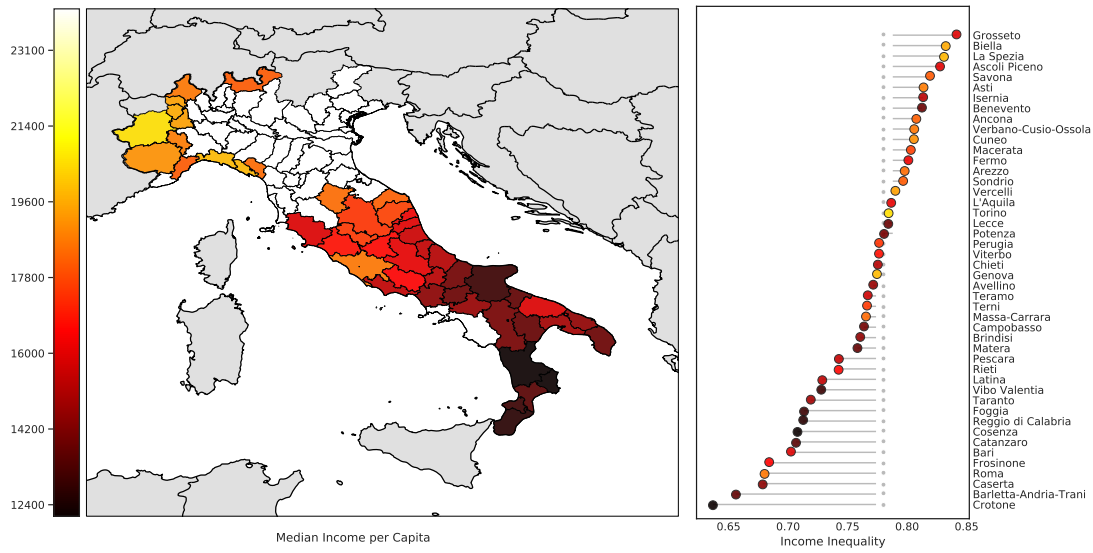
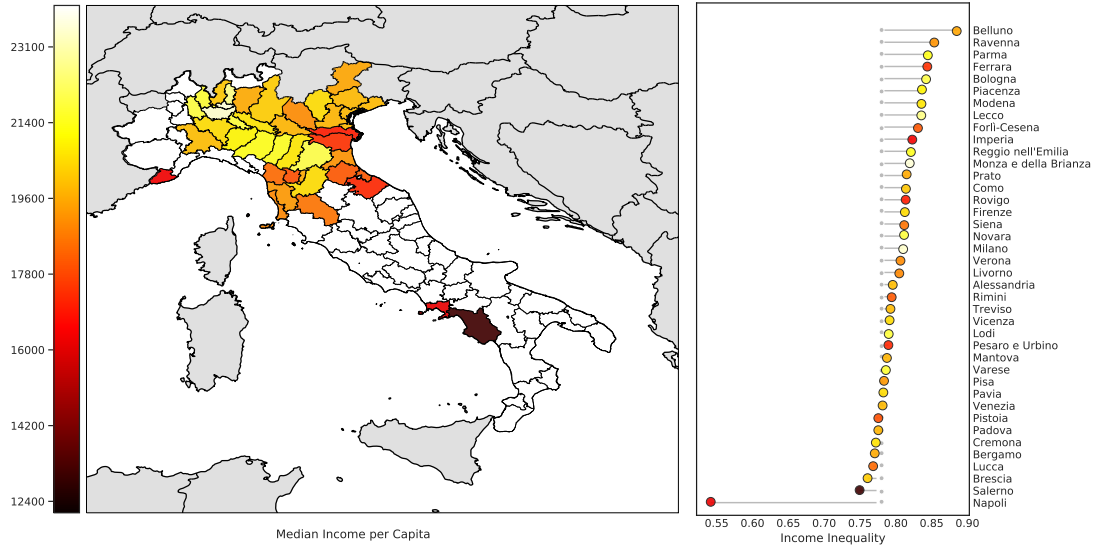


Figure 3: Correlation of mobility reduction and economic indexes.

Plot of the relative change in Nodal Efficiency, between pre- and post- lockdown values for each municipality, versus two different economic indexes, respectively Deprivation Index (top) and Irpef per Capita (bottom, x-axis in logarithmic scale). For each figure we provide two linear regression lines, one computed on the entire data (in blue) and one computed after filtering outliers w.r.t the economic index (in orange, using the 95-percentile as threshold). To ease the visualization, we draw the scatterplot by grouping points into 40 discrete bins, and showing mean and 95% confidence interval of each bin. Correlations are respectively significantly negative (Pearson: $R = -0.153, P \sim 0$; S-R: $R = -0.235, P \sim 0$; T-S: $R = -0.064$; K-T: $R = -0.162, P \sim 0$) and significantly positive (Pearson: $R = 0.263, P \sim 0$; S-R: $R = 0.404, P \sim 0$; T-S: $R = 0.001$; K-T: $R = 0.273, P \sim 0$).



(a) Most affected provinces (stronger decrease in Efficiency with respect to the median value)



(b) Least affected provinces (weaker decrease in Efficiency with respect to the median value)

Figure 4: Characteristics of the most affected (top panel) and the least affected (bottom panel) provinces. Left inset: geographic distributions with colors corresponding to median Income per Capita in every province. Right inset: position of each province in the distribution of Income Inequality with respect the average inequality in the sample (gray dotted line). Italian regions with not available data have been greyed out.

q	intercept	income pc	deprivation	fiscal capacity	inequality	real estate pc	(pseudo)R2
0.05	-0.8398*** (0.0491)	0.2587*** (0.0253)	0.1686*** (0.0276)	-0.1461*** (0.0286)	-0.0344* (0.0204)	-0.1622*** (0.0251)	0.05223
0.1	-0.5089*** (0.0456)	0.2871*** (0.0260)	0.1723*** (0.0266)	-0.1280*** (0.0261)	-0.0315* (0.0177)	-0.2539*** (0.0232)	0.17578
0.2	-0.2241*** (0.0317)	0.2272*** (0.0187)	0.1272*** (0.0179)	-0.0972*** (0.0242)	-0.0410*** (0.0124)	-0.2907*** (0.0206)	0.29896
0.8	0.3770*** (0.0199)	0.0788*** (0.0121)	0.0068 (0.0117)	-0.0548*** (0.0123)	0.0018 (0.0094)	0.0868*** (0.0133)	0.14346
0.9	0.8644*** (0.0523)	-0.0962*** (0.0347)	-0.0868*** (0.0319)	-0.3598*** (0.0335)	0.2099*** (0.0269)	0.8759*** (0.0304)	0.20012
0.95	1.2128*** (0.0761)	-0.2489*** (0.0542)	-0.1214** (0.0506)	-0.3844*** (0.0362)	0.3488*** (0.0329)	1.0334*** (0.0345)	0.24347
OLS	0.1098* (0.0576)	0.0654** (0.0327)	0.0557* (0.0328)	-0.2045*** (0.0404)	0.0737*** (0.0239)	0.1145*** (0.0398)	0.09001

Table 1: Results for quantile regression of the relative difference of efficiency over time with respect to income per capita with multiple controls: social and financial distress in the municipality (deprivation and fiscal capacity), concentration of estates (real estate pc), income inequality and regional controls (extended model). Regression obtained with the Iterative Weighted Least Squares method on standardized variables. Standard errors reported in parenthesis calculated via bootstrap with 1000 iterations. Pseudo R2 obtained via McFadden's method. Only quantile 5-20 and 80-95 shown, full results available upon request. Bottom line shows OLS regression as reference. Number of observations: 2345. Not shown: coefficients of 19 regional controls.

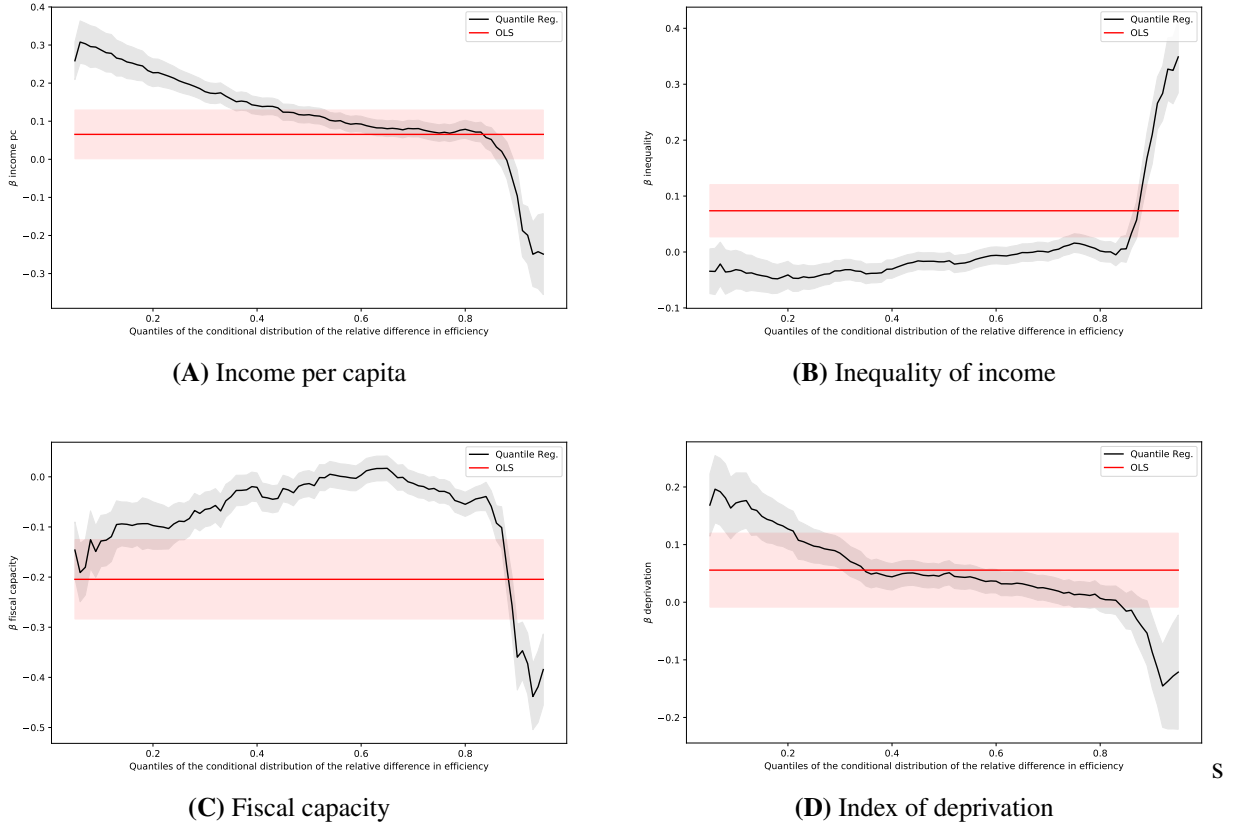


Figure 5: Regression coefficients by quantile for the extended model.

Plot of the regression coefficients for each percentile of the relative change in nodal efficiency over time for three of the main independent variables: Income per Capita (A), income Inequality (B), Fiscal capacity (C), Index of Deprivation (D). For each figure the coefficient of the quantile regression is plotted in black lines with bootstrapped confidence intervals at 95%, as a reference the OLS regression of the same variables is plotted in red.

Supplementary material for: Economic and social consequences of human mobility restrictions under COVID-19

Giovanni Bonaccorsi¹, Francesco Pierri², Matteo Cinelli³, Francesco Porcelli⁴, Alessandro Galeazzi⁵, Andrea Flori¹, Ana Lucia Schmidt⁶, Carlo Michele Valensise⁷, Antonio Scala³, Walter Quattrociocchi⁶, Fabio Pammolli^{1,8}

¹ Impact, Department of Management, Economics and Industrial Engineering, Politecnico di Milano

² Department of Electronics, Information and Bioengineering, Politecnico di milano

³ CNR-ISC

⁴ Department of Law, Università di Bari

⁵ Department of Information Engineering, Università di Brescia,

⁶ Department of Environmental Sciences, Informatics and Statistics, Università Ca'Foscari di Venezia

⁷ Department of Physics, Politecnico di Milano

⁸ CADS, Joint Center for Analysis, Decisions and Society, Human Technopole,

*To whom correspondence should be addressed; E-mail: giovanni.bonaccorsi@polimi.it

Materials and Methods

Data Collection

We analyzed mobility between municipalities based on “Movement Maps” provided by Facebook through its “Data For Good” program (1). These maps consist of de-identified and aggregated information of Facebook users retrieved by their mobile phones with geo-positioning enabled, showing movement across administrative regions (i.e. Italian municipalities in our case). Similar to recent research (2–4), data do not indicate numbers of individuals traveling but it is constructed by Facebook with proprietary methods, which include mechanisms to

ensure privacy protection (5), to provide an index that correlates with real movements of people (1). We collected data relative to movements between Italian municipalities from February 23rd to April 4th (COVID-19 was first diagnosed in the peninsula in the night between February 20th and February 21st). The resulting dataset contains approx. 800k distinct observations covering almost 3k distinct municipalities. The average number of daily users with location enabled during the observation period was approximately 3.8 million users, which is about 20 times higher than the panel of users analyzed in a similar work (6). In this work we built several mobility networks (aggregating flows over different periods of interest) as directed weighted graphs where nodes are municipalities and each arc represent the amount of population moving from origin to destination in a given time interval.

Data consistency check

We leverage a dataset which is constructed by Facebook with proprietary methods. In particular, the amount of people travelling between two locations in a given time interval is provided in two forms: a “baseline” value, that is computed as the average over the 45 days preceding day 0 of collection (February 23rd in our case), and a “crisis” value that corresponds to near real-time data (1). A measurement is retained only if the baseline value exceeds 10, otherwise it is discarded. This explains in the first place why we get mobility data only for $\sim 1/3$ of overall Italian municipalities. In light of this, we performed a robustness check to ensure that data provides an adequate level of representativity for the real mobility between municipalities. We assessed the amount of links we might be missing due to Facebook processing pipeline by computing the number of paths for which we have at least one daily observation depending on a given threshold applied on the baseline value. In Fig. 1a-b we show boxplots for the distribution of path coverage, respectively in the period before (February 23th-March 8th) and after (March 10th, April 04th) the day of lockdown, i.e., for each edge we compute the percentage of days

(over the entire period of observation) where we have a measurement. Missing values could be due either because their value is lower than 10 or because Facebook erroneously discarded them. We also consider edges increasingly based on their value (and filtering them according to increasing thresholds). We notice that before lockdown the median coverage is always above 75%, whereas values are slightly smaller for the period after lockdown (especially when considering smaller edges), most likely because of the effective reduction in mobility. We thus assume that the data collection is homogeneous in time and representative enough for the sake of our analysis.

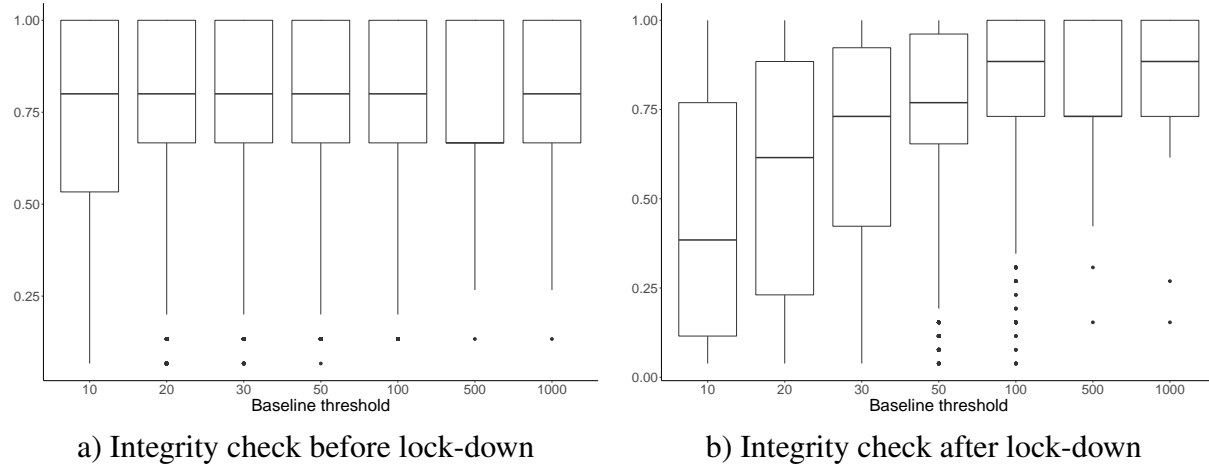


Figure 1: Integrity check for Facebook data before and after lock-down.

We show on the x-axis the baseline threshold we use to filter edges and on the y-axis the coverage percentage for each resulting set of edges. We perform this exercise for two periods, respectively: a) Feb 23rd-March 8th, and b) March 10th-April 04th.

Comparison with ISTAT baseline

We further evaluated the quality of Facebook mobility data by comparing it with a baseline dataset provided by the Italian National Institute of Statistics (ISTAT). This consists of a commuting network of workers/students travelling between municipalities, that was recorded with the last national census (2011). Such comparison has indeed a few caveats—it only tracks res-

idents who declared to be travelling for work/study and it is 9 years old—but we believe it is useful to further validate the situation of Italian mobility before lockdown. We performed a few adjustments in order to make a consistent comparison. First, we filtered out those paths where the number of travelers is less than 10 (as mentioned before, Facebook uses this value as threshold to include a measurement). Second, we retained only municipalities which are present in our data. For what concerns pre-lockdown mobility, we build an averaged graph over the 15 days before national lockdown, i.e. each edge has a weight which is the average of all the observations in that period. In both cases we filter self-loops which are ignored in our analyses. We obtain 2955 nodes and respectively 30,358 edges for the ISTAT network against 17,553 edges in our network. We find a significant positive correlation between Facebook and ISTAT Degree centrality distributions: Pearson $R = 0.80$, $P \sim 0$; Spearman-Rho $R = 0.64$, $P \sim 0$. We also find a significant positive correlation between Facebook and ISTAT edge weights (those are common to both graphs): Pearson: $R = 0.55$, $P \sim 0$; Spearman-Rho: $R = 0.37$, $P \sim 0$.

Network Efficiency

The efficiency is a global network measure that combines the information deriving from the network cohesiveness and the distance among the nodes. It measures how efficiently information is exchanged over the network (7) and it can be defined as the average of nodal efficiencies e_{ij} among couples of vertices of the network. Given a weighted network $G(V, E)$ with $n = |V|$ nodes and $m = |E|$ edges, the connections of G are represented by the weighted adjacency matrix W with elements $\{w_{ij}\}$ where $w_{ij} \geq 0 \forall i, j$. The global efficiency can be written by means of the following expression:

$$E_{glob}(G) = \frac{1}{n(n-1)} \sum_{i \neq j \in V} e_{ij} = \frac{1}{n(n-1)} \sum_{i \neq j \in G} \frac{1}{d_{ij}} \quad (1)$$

where d_{ij} is the distance between two generic nodes i and j , defined as the length of the shortest path among such nodes. The shortest path length d_{ij} is the smallest sum of the weights w_{ij}

throughout all the possible paths in the network from i to j . When node i and j cannot be connected by any path then $d_{ij} = +\infty$ and $e_{ij} = 0$. Following the methodology of (7), the global efficiency $E_{glob}(G)$ is normalized in order to assume maximum value $E(G) = 1$ in the case of perfect efficiency. To normalize $E_{glob}(G)$, we consider the case of the ideal network G_{id} , that is a fully connected graph, where all nodes are connected to each other via the shortest possible distance that, in our case, corresponds to $\min(d_{ij}) = \min(w_{ij}) = w_{\min} \forall i, j$. The efficiency of such ideal graph is $E_{glob}(G_{id}) = 1/w_{\min}$ and thus the normalized efficiency is $E(G)_{norm} = E_{glob}(G)/E_{glob}(G_{id})$ with range $0 \leq E(G)_{norm} \leq 1$. In such a setting the nodal efficiency, i.e. the contribution of each node to the global efficiency, can be simply written as:

$$e_i = \frac{1}{n-1} \sum_{j \neq i} \frac{1}{d_{ij}} \quad (2)$$

while the normalized nodal efficiency can be written as $e_i^{norm} = e_i w_{\min}$.

Facebook mobility graph is a directed weighted network in which two municipalities A and B are connected by (directed) edges weighted by the sum of a de-identified and aggregated index which correlates with people movements from origin A to destination B (1). Beside the geographical distance between two nodes of the graphs, an epidemiological proximity can also be defined, considering that two locations are closer if many people move between them. To compute network efficiency in our case we invert the weight of each link and consider as distance the sum of the weights along the path connecting two nodes. In case multiple paths are possible, the one with the minimum total weight, corresponding to the shortest path, is considered.

Centrality measures

We computed the distribution of several node centrality measures for four different snapshots of the Italian mobility network of municipalities. Each snapshot was taken over a distinct window

of 7 days, respectively from Feb 23rd to Feb 29th, from March 1st to March 7th, from March 8th to March 14th and from March 15th to March 21st.

We observed a significant change in the distributions across time for all measures, as shown in Figs 1-8, where we provide the Complementary Cumulative Distribution function for each week. We provide in Table 1 applications of Kruskal-Wallis test and post-hoc multiple comparison Dunn's test (with Holm's p-value adjustment).

Centrality	Kruskal-Wallis	P-value pairwise tests for different weeks					
		W1 W2	W1 W3	W1 W4	W2 W3	W2 W4	W3 W4
Degree	478.72***	7.62E-01	3.71E-07	3.39E-80	1.24E-06	8.89E-78	1.55E-42
In-Degree	471.44***	8.04E-01	1.73E-07	6.97E-79	4.49E-07	6.16E-77	8.97E-41
Out-Degree	451.76***	6.99E-01	1.60E-06	5.29E-76	7.39E-06	5.42E-73	4.08E-41
Strength	767.54***	5.02E-01	8.48E-24	5.09E-129	4.41E-21	4.01E-122	2.19E-44
In-Strength	761.47***	5.43E-01	9.35E-24	1.19E-127	2.67E-21	2.00E-121	1.19E-43
Out-Strength	724.49***	4.96E-01	9.08E-23	5.96E-122	4.42E-20	3.69E-115	1.09E-41
Clustering Coefficient	89.11***	2.21E-01	5.53E-03	5.45E-18	2.21E-01	2.07E-12	3.98E-08
Nodal Efficiency	2811.91***	1.41E-11	3.64E-119	0.00E+00	7.39E-61	0.00E+00	1.43E-141

Table 1: Application of Kruskal-Wallis and post-hoc Dunn's multiple test comparison (with Holm's pvalue adjustment).

We performed for each centrality measures a Kruskal-Wallis test to assess that the four weekly distributions are significant different (** means significant at alpha=0.001) and then we performed a multiple pair-wise comparison test using Dunn's procedure with Holm's p-value adjustments.

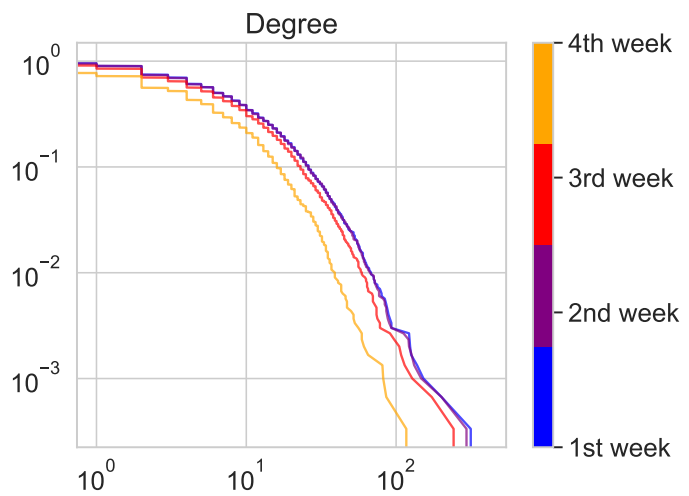


Figure 2: Distribution of Degree centrality across 4 consecutive weeks.

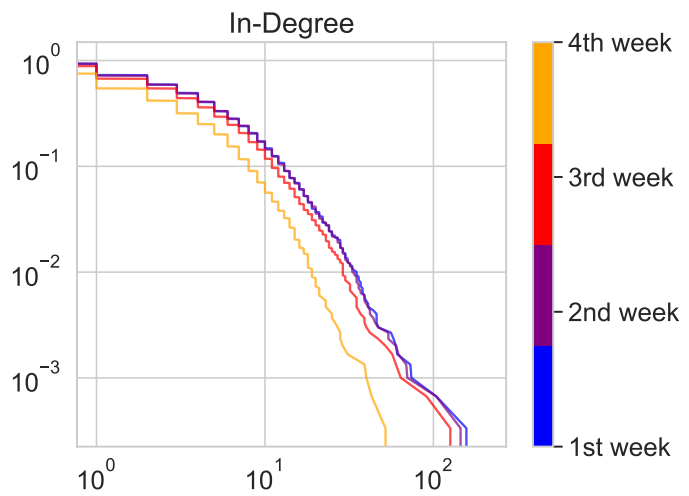


Figure 3: Distribution of In-Degree centrality across 4 consecutive weeks.

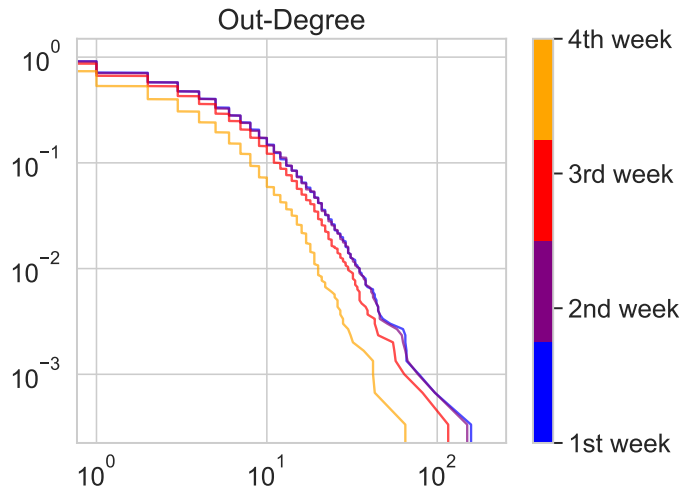


Figure 4: Distribution of Out-Degree centrality across 4 consecutive weeks.

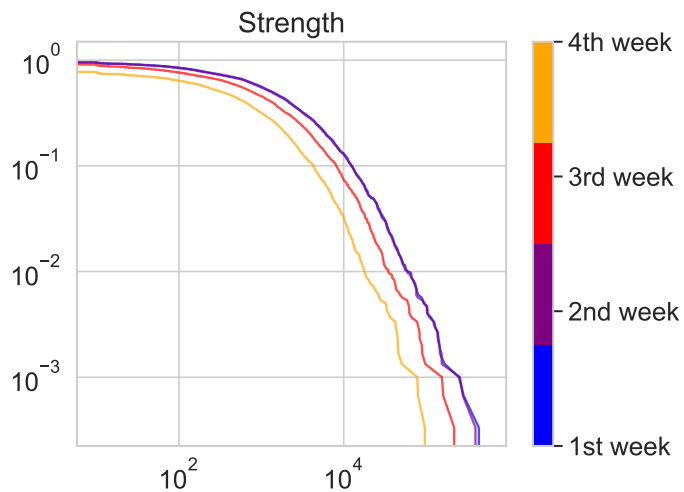


Figure 5: Distribution of Strength centrality across 4 consecutive weeks.

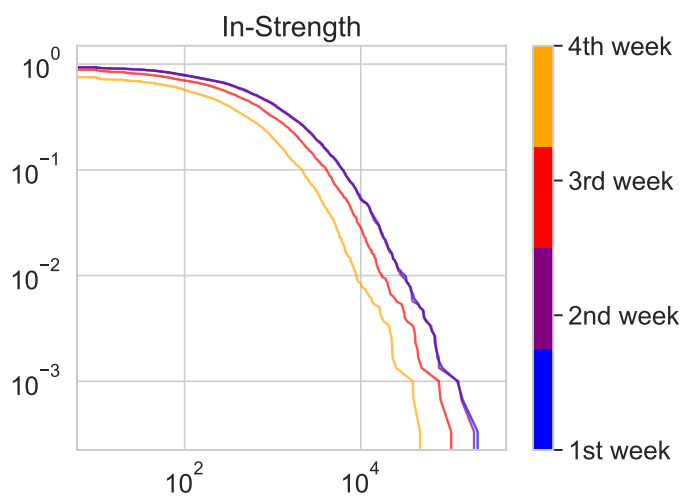


Figure 6: Distribution of In-Strength centrality across 4 consecutive weeks.

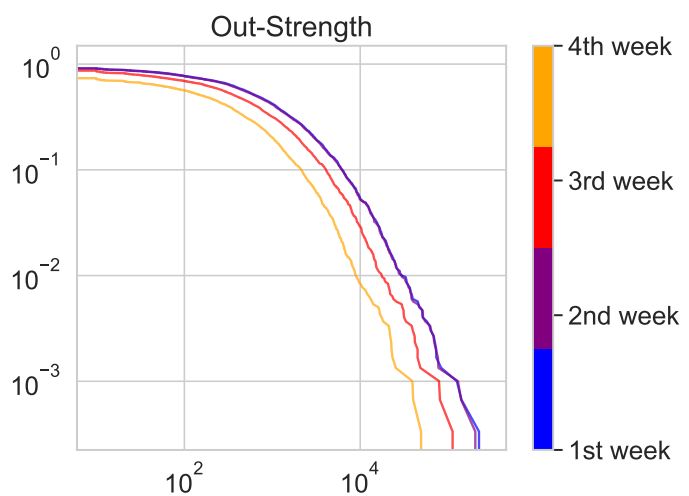


Figure 7: Distribution of Out-Strength centrality across 4 consecutive weeks.

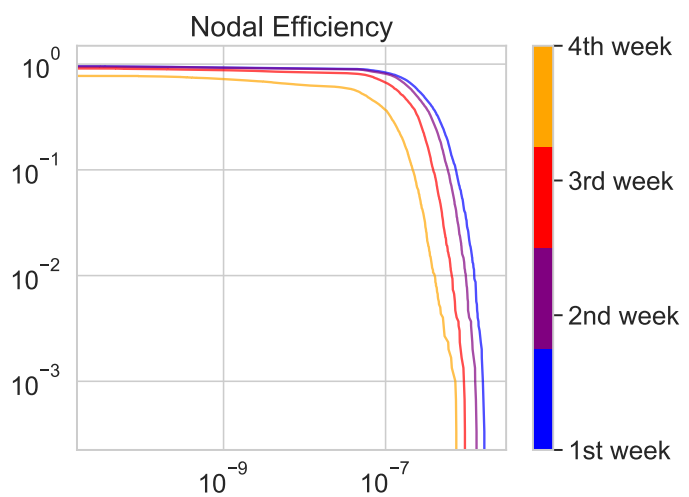


Figure 8: Distribution of Nodal Efficiency across 4 consecutive weeks.

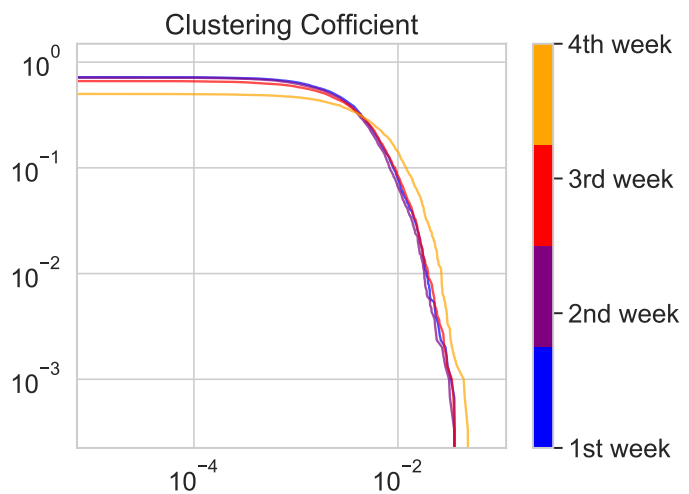


Figure 9: Distribution of Clustering Coefficient across 4 consecutive weeks.

Correlation between variation in Nodal Efficiency, Degree and Strength

We show in Table 2 an application of Pearson, Spearman-Rho, Theil-Sen and Kendall's Tau test to assess the correlation between relative change (in percentage) between Nodal Efficiency vs Degree and Strength node centralities. We also show two relative scatter plots with a linear regression line (Figs 10 and 11).

Centrality	Pearson	Spearman-Rho	Theil-Sen	Kendall's Tau
Degree	R=0.61 P=4.35E-300	R=0.63 P=7.10E-320	R=0.63	R=0.47 P=1.17E-303
Strength	R=0.51 P=1.42E-194	R=0.45 P=7.80E-146	R=0.65	R=0.33 P=8.96E-149

Table 2: Correlation tests between relative change (in percentage) in Nodal Efficiency vs Degree and Strength.

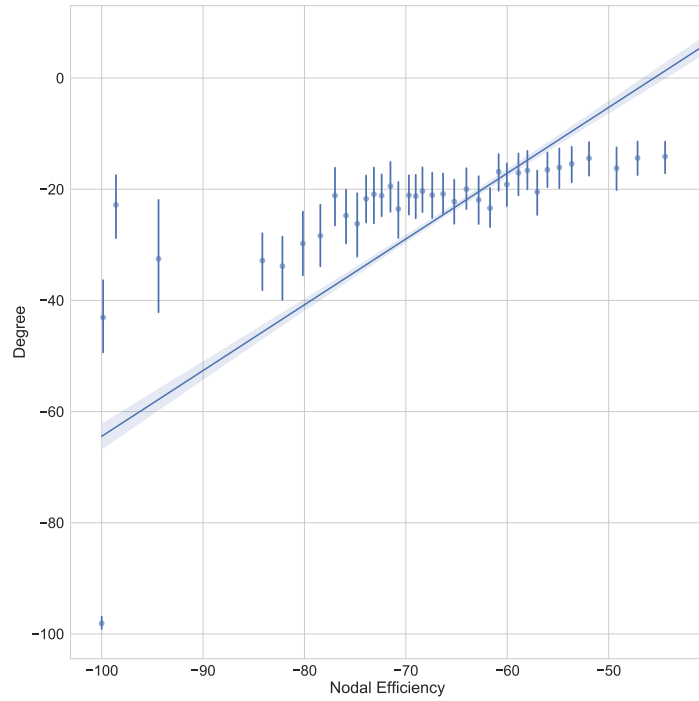


Figure 10: Scatterplot of relative change in Nodal Efficiency vs Degree. We group data points in 40 bins to ease visualization. We also show a linear fitting.

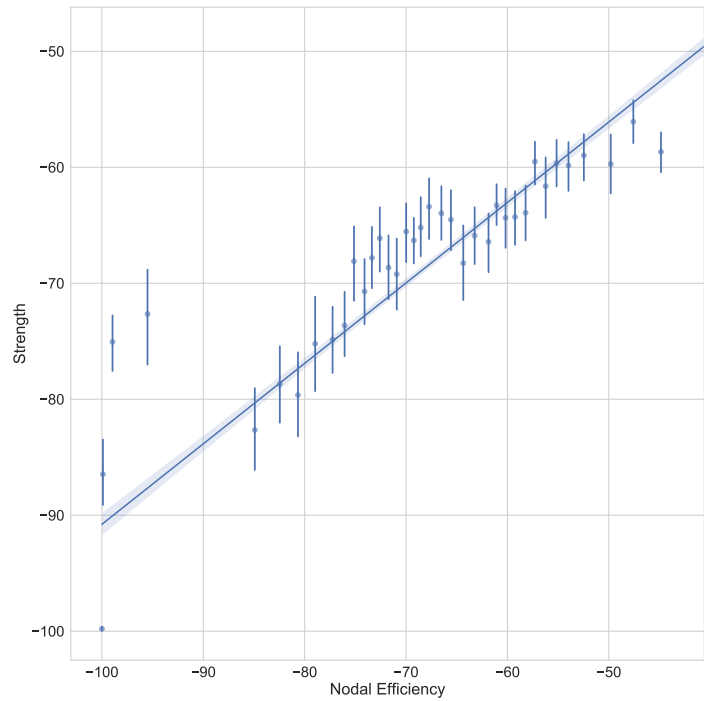


Figure 11: Scatterplot of relative change in Nodal Efficiency vs Strength. We group data points in 40 bins to ease visualization. We also show a linear fitting.

Joint distribution of mobility and economic data

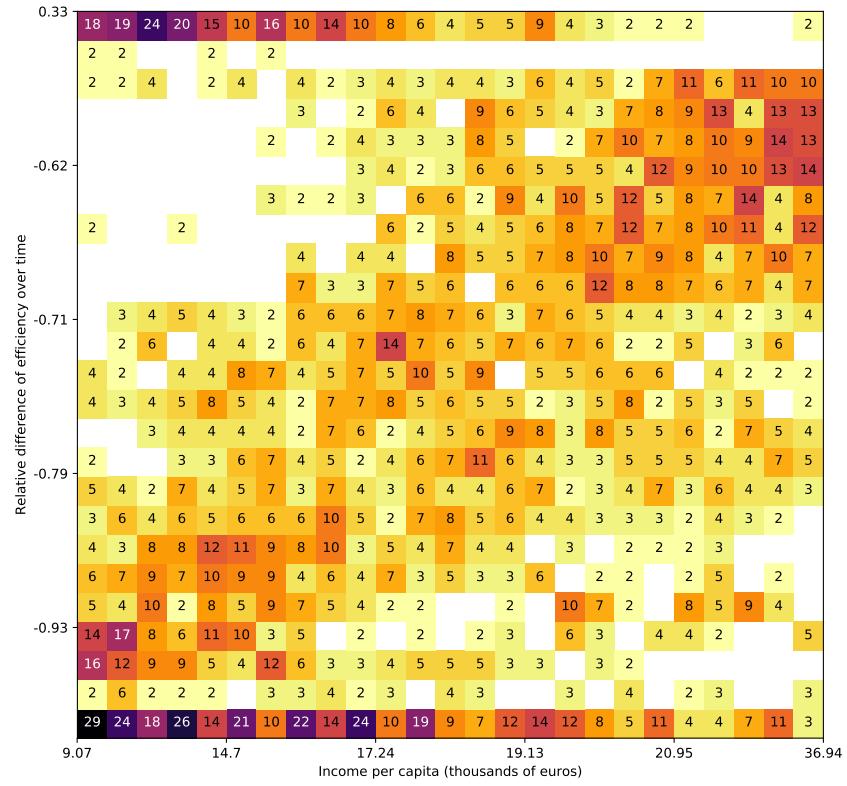


Figure 12: Joint distribution by percentile of income and change in efficiency over time.

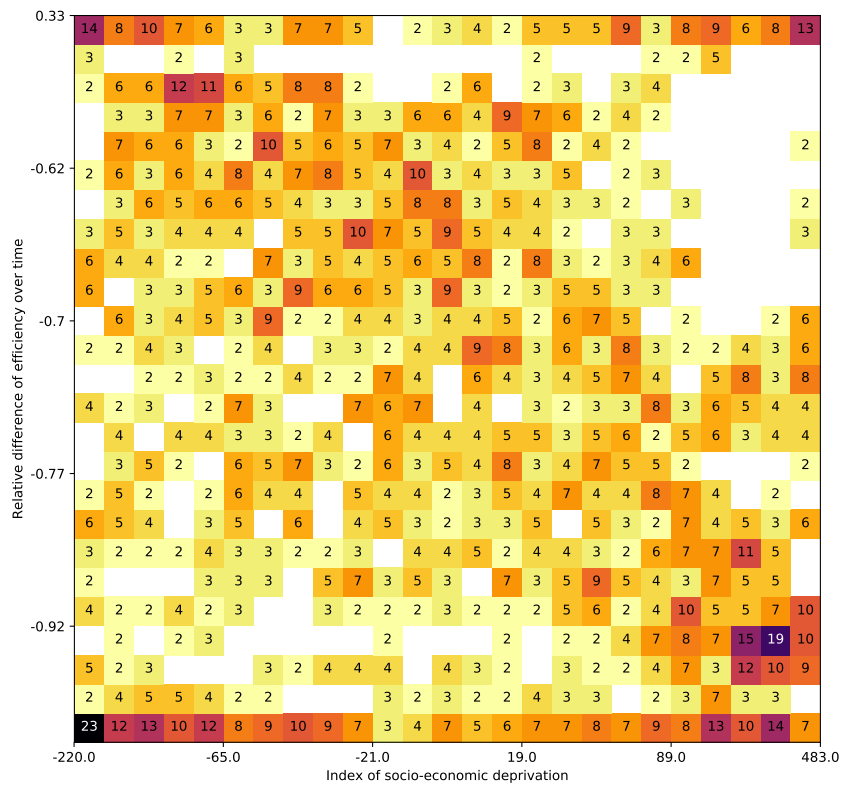


Figure 13: Joint distribution by percentile of deprivation index and change in efficiency over time.

Economic model

Let us denote t_0 as the 14 days period before lockdown and t_1 as the 14 days period after lockdown. We construct two networks of mobility for each of the periods t_0 and t_1 , where nodes are represented by municipalities and (weighted) edges correspond to the sum of mobility traffic between them over time, as measured by Facebook. In our sample, we define the relative variation in efficiency e_i as $\frac{e_{i;t_1} - e_{i;t_0}}{e_{i;t_0}}$ where e_i is defined as in 2.

For our economic model we estimate the following equation:

$$e_i = \beta + x_i + z_i \quad (3)$$

Where x_i is a vector of economic indicators measured at municipal level and z_i presents a matrix of regional fixed effects. All economic indicators have been measured for periods preceding the start of the lockdown and are described below.

Economic and structural data

Economic and structural information cover different dimensions of the local socioeconomic context of each Italian municipality, in total 7904 jurisdictions, representing the smallest administrative unit in Italy and the closest proxy to individual information available in official statistics.

In total our data-set includes six variables: individual average declared income, a proxy of the wellbeing of citizens; deprivation, fiscal capacity and inequality provide different measures of the municipal financial and social wealth; finally, as a proxy of the structural features of each territory, we include the number of real estates per capita and regional fixed effects.

Declared income

This variable is the tax base of the personal income tax declared by tax payers in the 2018 tax return to the Revenue Agency for the 2017 financial year, the distribution at municipal level is provided by the Ministry of Economic and Finances (MEF), and both the mean and the median values are included in the dataset.

Municipal index of socioeconomic deprivation

This variable is a composite index made up of five elementary indicators that cover the following dimensions:

- Education: the percentage of population older than 6 years which is illiterate or without a degree;
- Unemployment: the percentage of active population without a job;
- Housing: the percentage of rented properties over the total number of real estate properties;
- Population density: average number of components in each family;
- Economic poverty: percentage of taxpayers with a total declared income lower than 10,000 euros.

The five elementary indicators are computed at municipal level, then transformed in percentage deviation from the national mean, and finally aggregate together with equal weights. The aggregation methodology is reported ⁸⁾. (This index is one of the main determinants of municipal standard expenditure needs. The data are made available by the Italian MEF through the website Opencivitas.it (a repository of all information used for the evaluation of municipal standard expenditure needs)).

Municipal fiscal capacity

This variable is the official measure of the standard level of municipal fiscal revenues based on three main sources: property tax, local income tax, and local fees. This value, based on 2016 data (latest available information), has been computed by the Italian MEF and represents, together with standard expenditure needs, the main building block of the Italian system of municipal fiscal equalization. Official figures are made public each year through a specific decree.

Municipal income inequality

We measure income inequality at municipal level in a very simply and direct way as the ratio between average and median values of the distribution of the declared income. Municipalities with values above 1 are those where income is less equally distributed.

Number of real estates per capita

This is the number of existing buildings of all categories divided by the number of individuals in the municipality, this variable can be interpreted as inverse measure of population density or as a direct measure of urban sprawl. Data are available through ISTAT for the year 2016 (latest available information).

Regional controls

Our regression sample has a good representation of the entire set of Italian municipalities, both in terms of population size and geographical location, including 2387 observations corresponding to 30% of Italian municipalities. Nevertheless, to exclude spatial spillovers effect we control for regional confounding factors.

Correlation with centrality measures

We performed correlation exercises between the main economic indices of interest (declared income per capita and deprivation index) and aforementioned centrality measures (using relative change in percentage). We provide applications of Pearson and Spearman-Rho test (and Theil-Sen coefficient) in Table 2.

Centrality	Economic Index	Pearson	Spearman-Rho	Theil-Sen	Kendall's Tau
Irpef per Capita	In Degree	R=0.15 P=9.09E-16	R=0.07 P=1.96E-04	R=-0.00	R=0.05 P=2.49E-04
Irpef per Capita	In Strength	R=0.21 P=1.50E-29	R=0.29 P=1.45E-53	R=0.00	R=0.19 P=5.08E-53
Irpef per Capita	Out Degree	R=0.16 P=1.38E-17	R=0.08 P=3.76E-05	R=-0.00	R=0.05 P=5.53E-05
Irpef per Capita	Out Strength	R=0.23 P=2.90E-33	R=0.28 P=1.53E-50	R=0.00	R=0.19 P=3.49E-50
Irpef per Capita	Degree	R=0.18 P=1.20E-22	R=0.13 P=1.64E-11	R=0.00	R=0.09 P=3.90E-11
Irpef per Capita	Strength	R=0.23 P=1.37E-34	R=0.29 P=1.14E-57	R=0.00	R=0.20 P=2.69E-57
Deprivation Index	In Degree	R=-0.07 P=5.54E-04	R=-0.12 P=4.99E-09	R=-0.05	R=-0.09 P=1.66E-09
Deprivation Index	In Strength	R=-0.05 P=1.13E-02	R=-0.09 P=1.10E-05	R=-0.02	R=-0.07 P=3.33E-06
Deprivation Index	Out Degree	R=-0.04 P=8.64E-02	R=-0.08 P=9.35E-05	R=-0.05	R=-0.06 P=3.73E-05
Deprivation Index	Out Strength	R=-0.03 P=1.59E-01	R=-0.06 P=4.05E-03	R=-0.02	R=-0.04 P=1.81E-03
Deprivation Index	Degree	R=-0.05 P=2.95E-02	R=-0.10 P=3.89E-06	R=-0.04	R=-0.07 P=1.18E-06
Deprivation Index	Strength	R=-0.04 P=7.78E-02	R=-0.07 P=8.22E-04	R=-0.03	R=-0.05 P=3.36E-04

Table 3: Correlation tests between several centrality measures and main economic indices used in our analysis.

References and Notes

1. P. Maas et al., Proceedings of the 16th International Conference on Information Systems for Crisis Response and Management (ISCRAM), Valencia, Spain.(2019).
2. M. Chinazzi,et al., Science(2020).
3. M. U. G. Kraemer et al., Science(2020).
4. A. Aleta, Q. Hu, J. Ye, P. Ji, Y. Moreno,medrxiv.org:2020.03.05.20031740 (05 March 2020)(2020).
5. C. O. Buckee et al., Science(2020).
6. E. Pepe et al., medrxiv:2020.03.22.20039933 (22 March 2020)(2020).
7. V. Latora, M. Marchiori,Physical review letters 87, 198701 (2001).
8. Soluzioni per il Sistema Economico S.p.a (SOSE), Revisione della metodologia dei fabbisogni standard dei comuni,http://www.mef.gov.it/ministero/commissioni/ctfs/documents/Nota_revisione_metodologia_FS2017SOSI3.settembre_2016.pdf (2016).